Stronski et al. Nanoscale Research Letters (2016) 11:39
DOI 10.1186/s11671-016-1235-x

Nanoscale Research Letters
a SpringerOpen Journal

NANO EXPRESS Open Access

Holographic and e-Beam Image Recording in $Ge_5As_{37}S_{58}$–Se Nanomultilayer Structures

A. Stronski[1], E. Achimova[2], O. Paiuk[1*], A. Meshalkin[2], V. Abashkin[2], O. Lytvyn[1], S. Sergeev[2], A. Prisacar[2] and G. Triduh[2]

Abstract

Processes of e-beam and holographic recording of surface relief structures using $Ge_5As_{37}S_{58}$–Se multilayer nanostructures as registering media were studied in this paper. Optical properties of $Ge_5As_{37}S_{58}$, Se layers, and $Ge_5As_{37}S_{58}$–Se multilayer nanostructures were investigated. Spectral dependencies of refractive index were analyzed within the frames of single oscillator model. Values of optical band gaps for $Ge_5As_{37}S_{58}$, Se layers, and $Ge_5As_{37}S_{58}$–Se multilayer nanostructures were obtained from Tauc dependencies. Using e-beam and holographic recording, diffraction gratings were fabricated in $Ge_5As_{37}S_{58}$–Se multilayer nanostructures. Images of Ukraine and Moldova state emblems were obtained by e-beam recording. Image size consisted of 512 × 512 pixels (size of 1 pixel was ~2 μm). $Ge_5As_{37}S_{58}$–Se multilayer nanostructures are perspective for the direct recording of holographic diffraction gratings and other optical elements.

Keywords: Multilayer nanostructures, Holographic recording, e-beam recording, Diffraction gratings, Chalcogenide glasses

Background

Thin films based on chalcogenide glasses have evolved as light-sensitive materials for high-density recording media application due to their optical and structural properties. The light sensitivity effect of thin chalcogenide films was discovered 50 years ago [1]. Chalcogenide glasses and films are also sensitive to the electron or ion beams, X-rays [2–5], and perhaps photo-stimulated or stimulated by electron or ion beams; X-rays' change of their properties is the most interesting phenomena exhibited by these materials.

In this work, the experimental results showing the surface relief formation in $Ge_5As_{37}S_{58}$–Se nanomultilayer structures under e-beam or holographic exposure are presented.

Selective etching after exposure enables to obtain surface reliefs and to use media such as high-resolution inorganic resists [2–7]. Using of thin layers of chalcogenide glasses as high-resolution media and selective etching after exposure enables fabrication of high-quality holographic diffraction gratings and other optical elements [6–11].

Multilayer nanostructures on the base of chalcogenide glasses and the possibility to use them as registering media were proposed in [12]. Such media do not require the step of selective etching for the formation of the surface relief [12–16]. Surface relief in such media is formed directly during exposure process. Absence of the selective etching step is the advantage of such media because often USED etchants are toxic, and during selective etching process, it is necessary to control many parameters (temperature, concentration of etchant, etc.). Thus, the development of one-step method for the fabrication of surface reliefs is considered perspective for the fabrication of planar optical elements.

Chalcogenide glasses of Ge–As–S composition are characterized by high values of refractive index, and their nonlinear optical properties are two orders higher than characteristic of quartz glasses [17, 18]. Earlier, we demonstrated the possibility to use $Ge_5As_{37}S_{58}$–Se multilayer nanostructures for the fabrication of surface reliefs [15]. In present work, results of direct recording (without the selective etching step) of holographic diffraction grattings and images by e-beam exposure using $Ge_5As_{37}S_{58}$–Se multilayer nanostructures as recording media are presented.

* Correspondence: paiuk@ua.fm
[1]V. Lashkaryov Institute of Semiconductor Physics, National Academy of Science of Ukraine, 41 Nauki ave., Kiev 03039, Ukraine
Full list of author information is available at the end of the article

Methods

Bulk glasses of $Ge_5As_{37}S_{58}$ were fabricated by common melt quenching method [15, 17, 18]. Amorphous $Ge_5As_{37}S_{58}$–Se nanomultilayers were prepared by computer-driven cyclic thermal vacuum deposition from two isolated boats with $Ge_5As_{37}S_{58}$ and Se on constantly rotated glass substrate with deposited ITO layer at room temperature in one vacuum deposition cycle (Fig. 1).

The control of the film thickness was carried out in situ during the thermal evaporation by interference thickness sensor at $\lambda = 0.95$ μm. Scheme of transverse cross section of the sample is shown in Fig. 2, where 1 is the glass substrate, 2 $Ge_5As_{37}S_{58}$ layer deposited nanolayer by nanolayer, 3 $Ge_5As_{37}S_{58}$–Se multilayer nanostructure, and 4 Se layer deposited nanolayer by nanolayer.

Overlapping part of the sample consists of alternating Se and $Ge_5As_{37}S_{58}$ nanolayers; two wide rings are overlapping in the central part of the substrate forming the $Ge_5As_{37}S_{58}$–Se multilayer nanostructure. Consequently, external and inner rings of the layers are $Ge_5As_{37}S_{58}$ and Se layers. $Ge_5As_{37}S_{58}$ and Se were deposited through mask windows. The substrate with deposited multilayer structure and $Ge_5As_{37}S_{58}$ and Se layers was used for the composition control and also for AFM thickness measurement and estimation of modulation period N (common thickness of one $Ge_5As_{37}S_{58}$ nanolayer and one Se nanolayer) of multilayer nanostructure. Overlapping part of the samples (see Fig. 2.) contains alternating nanolayers of $Ge_5As_{37}S_{58}$ with thickness of 16 nm and Se nanolayers with thickness of 14 nm. The total number of nanolayers was 200, modulation period $N \sim$ 30 nm. In order to prevent crystallization of Se layers which are structurally unstable under heating and/or exposure by light, e-beams, etc., heating of layers was minimized by substrate rotation and lowered evaporator temperature.

Optical properties of fabricated films and structures were investigated with the use of optical transmission spectra measured at normal light incidence. Transmission spectra (Fig. 3) were measured in the 450–900-nm range with the use of Specord M40 spectrophotometer for obtaining thickness, optical band gap, and spectral dependencies of refractive index of $Ge_5As_{37}S_{58}$, Se layers, and $Ge_5As_{37}S_{58}$–Se multilayer nanostructure.

Recording of holographic gratings was carried out with the use of DPSS laser radiation on 532 nm wavelength; diffraction efficiency of the diffraction gratings was controlled during recording process using 650 nm wavelength. Recording scheme is shown in Fig. 4.

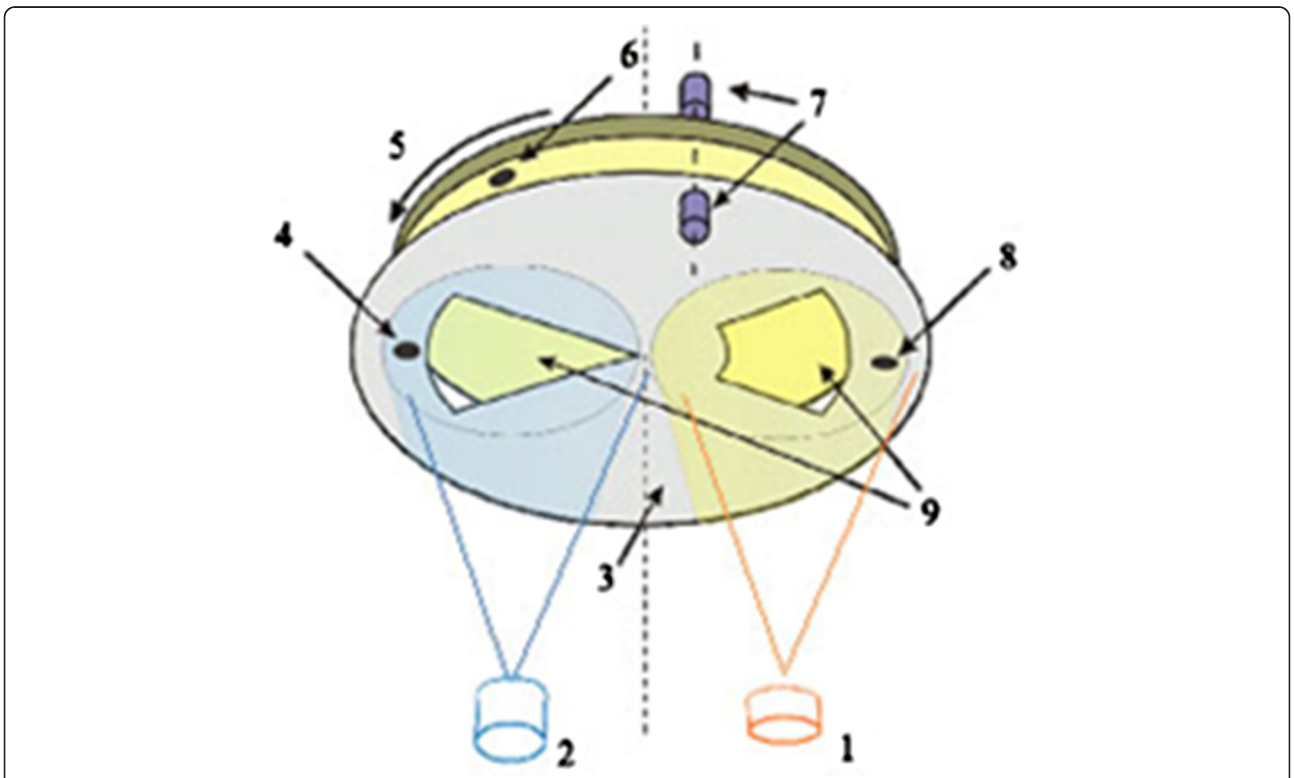

Fig. 1 Scheme of device for fabrication of multilayer nanocomposites on the base of chalcogenide glasses. *1* Evaporate of Ge-As-S chalcogenide glass, *2* evaporator of Se, *3* stationary mask, *4* and *8* quartz thickness sensors fixed on mask, *5* rotating samples holder, *6* quartz thickness sensor fixed on the rotating samples holder, *7* optical fibers of spectrophotometer, *9* windows in mask

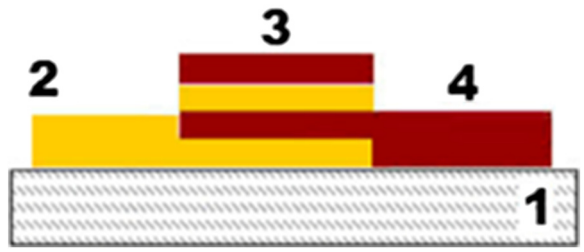

Fig. 2 Scheme of the sample structure. *1* Glass substrate, *2* $Ge_5As_{37}S_{58}$ layer, *3* $Ge_5As_{37}S_{58}$–Se multilayer nanostructure, *4* Se layer

Diffraction gratings of Ukrainian and Moldavian state emblems were recorded by e-beam exposure using scanning electron microscope Tesla BS 300 with programmable exposure control unit. The accelerating voltage was 25 kV, and the size of the electron spot at this voltage was about 300 nm. Size of images consisted of 512 × 512 pixels. Morphology and surface relief of the obtained images were studied by AFM microscopy. Distance between pixels consisted of 3 μm. Size of pixels was about 2 μm and profile depth ~300 nm.

Results and Discussion

The refractive index, n, and the film thickness were calculated using Swanepoel's method [19]. Algorithms and computer program for the calculation of envelope curves and refractive index were similar to those presented in [20–23]. The method allows the calculation of n when both the refractive index of the substrate and the position of the interference extrema are known. In the present study, the refractive index, s, of the substrate was determined independently at various wavelengths by measuring the transmittance, T_s, of the substrate alone (see curve 4 Fig. 3) and using the following equation [24]:

$$s = 1/T_s + \left(T_s^2 - 1\right)^{1/2}. \quad (1)$$

For chalcogenide semiconductors, the optical absorption coefficient, α, changes rapidly for photon energies comparable to that of the band gap, E_g, giving rise to an absorption edge with three regions—for the largest electron energies, in the region of the edge itself ($10 < \alpha < 10^4$ cm^{-1}), and at the lowest photon energies [25]. The first one is for the highest values of the absorption coefficient ($\alpha \geq 10^4$ cm^{-1}) which corresponds to transitions between extended states in both valence and conduction bands where the power law of Tauc [26] is valid.

$$\alpha(h\nu) = \frac{B\left(h\nu - E_g\right)^2}{h\nu} \quad (2)$$

B is the slope of the Tauc edge which reflects some disorder of the samples. Usually, this constant depends on the width of the localized states in the band gap, a fact explained with the homopolar bonds' presence in the chalcogenide glasses. Thus, Tauc plots of $(\alpha h\nu)^{1/2}$ versus $(h\nu)$ should be linear and extrapolate to values of the optical gap, E_g.

The dispersion of the refractive index was analyzed using the Wemple–DiDomenico (WDD) model [27, 28], which is based on the single oscillator formula:

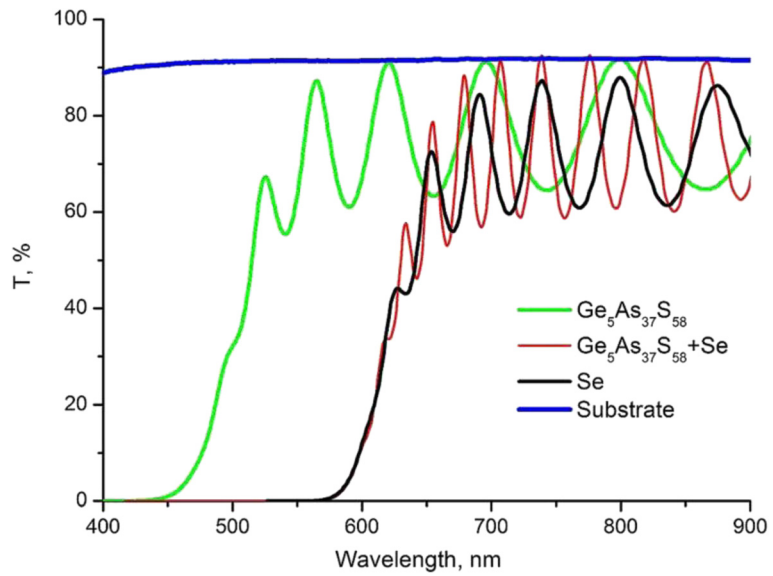

Fig. 3 Optical transmission spectra of $Ge_5As_{37}S_{58}$, Se layers, and $Ge_5As_{37}S_{58}$–Se multilayer nanostructure

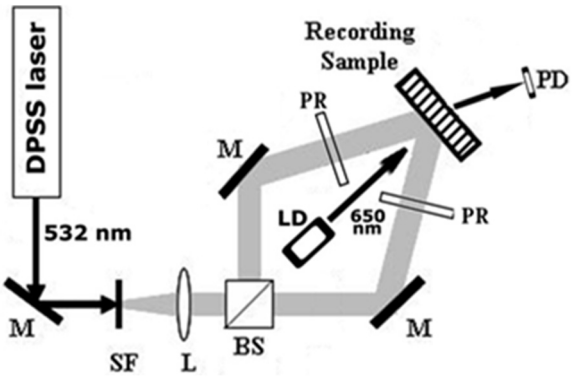

Fig. 4 Optical arrangement for holographic grating recording with real-time measurement of diffraction efficiency by photodetector. CW DPSS laser ($\lambda = 532$ nm, power =100 mW). *M* Mirror, *SF* spatial filter, *L* collimating lens, *BS* beam splitter, *LD* laser diode ($\lambda = 650$ nm) for monitoring recording process, *PR* polarization retarder, *PD* photodetector

$$n^2 - 1 = E_d E_0 / \left(E_0^2 - E^2\right), \quad (3)$$

where $(h\nu)$ is the photon energy, E_0 is the oscillator energy, and E_d is the oscillator strength or dispersion energy. The parameter E_d which is a measure of the intensity of the inter-band optical transition does not depend significantly on the band gap. By plotting $(n^2 - 1)^{-1}$ against $(h\nu)^2$ and fitting a straight line to the points, E_d and E_0 can be directly determined from the slope, $(E_d E_0)^{-1}$, and the intercept E_0/E_d on the vertical axis. The extrapolation for $(h\nu) \rightarrow 0$ also gives frequency-independent refractive index or the so-called static refractive index, n_0.

The dispersion energy is related to other physical parameters of material through the empirical formula:

$$E_d = \beta N_c Z_a N_e, \quad (4)$$

where N_c is the effective coordination number of the cation nearest neighbor to the anion, Z_a is the formal chemical valency of the anion, N_e is the total number of valence electrons per anion, and β is a constant (with a value depending on whether the solid is covalent or ionic, $\beta = 0.26 \pm 0.03$ and $\beta = 0.37 \pm 0.04$ eV, respectively). As found by Wemple and DiDomeniko [27], the

Table 1 Parameters of single oscillator model and values of optical band gap for $Ge_5As_{37}S_{58}$, Se films, and $Ge_5As_{37}S_{58}$–Se multilayer nanostructures

Layer composition	$n(0)$	E_d, eB	E_0, eB	E_g, eB
Se	2.28	19.09	4.53	1.91
$Ge_5As_{37}S_{58}$	2.24	18.29	4.57	2.27
$Ge_5As_{37}S_{58}$–Se	2.37	17.67	3.84	1.92

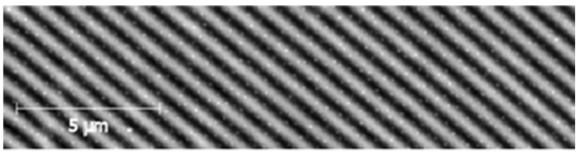

Fig. 5 AFM image of surface of holographic diffraction grating with spatial frequency 1000 mm^{-1}, obtained on the base of $Ge_5As_{37}S_{58}$–Se multilayer nanostructure

oscillator energy E_0 is closely related to the optical band gap energy E_g.

As can be seen from Fig. 3, absorption edge of $Ge_5As_{37}S_{58}$–Se multilayer nanostructures practically coincides with the absorption edge of Se (see also Table 1). It is necessary to note (see Fig. 3) high optical quality of $Ge_5As_{37}S_{58}$ layers and $Ge_5As_{37}S_{58}$–Se multilayer nanostructures (film transmission coincides with the substrate transmission in sites of interference maxima) and the presence of scattering in Se layer (transmission values of interference maxima for Se layers are smaller than values of substrate transmission).

The thicknesses of constituent $Ge_5As_{37}S_{58}$ and Se nanolayers were 16 and 14 nm, respectively, and are sufficiently smaller than the light wavelength. Also, transmission curve of $Ge_5As_{37}S_{58}$–Se multilayer nanostructure is a typical interference curve for films with high optical quality and uniform thickness (see Fig. 3). Thus, in the analysis of optical transmission spectra of nanomultilayer structure, it was possible to use the "effective optical medium" model: the layers with small optical band gap E_g value determine the optical absorption at the average absorption edge E_g, and the "barrier" layers with larger E_g are transparent.

Obtained spectral dependencies of refractive index of $Ge_5As_{37}S_{58}$, Se layers, and $Ge_5As_{37}S_{58}$–Se multilayer nanostructures were analyzed within the frames of single

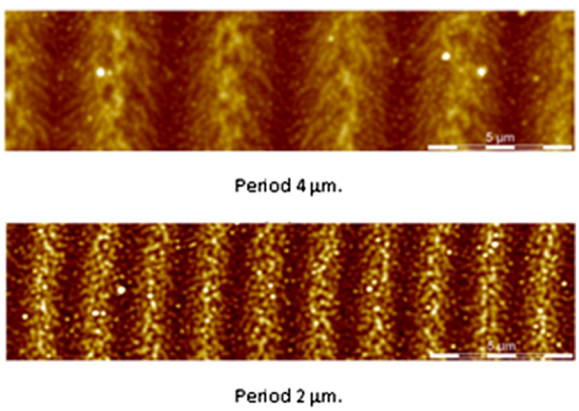

Fig. 6 Diffraction gratings obtained with the use of e-beam recording

oscillator model. Parameters of the model (dispersion energy, position of the effective oscillator) were obtained.

Parameters of single oscillator model dispersion energy and effective oscillator position and also values of optical band gap obtained with the use of Tauc dependence $\alpha h\nu = \text{const}(h\nu - E_g)^2$, where $h\nu$ is the light quantum energy, α absorption coefficient, and static refractive index, n_0, are presented in Table 1.

It is necessary to note that values of optical band gaps (see Table 1) of Se layers and $Ge_5As_{37}S_{58}$–Se multilayer nanostructure are close. The Wemple–DiDomenico model in the range of the low-frequency optical dielectric response of glasses can be used as a tool to probe the building blocks conforming a glass and allows quantitative analysis in combination with Raman spectroscopy [29].

Mechanism of recording in chalcogenide multilayer nanostructures is connected with stimulated by light (ion, electron beams) interdiffusion processes in nanolayers [30]. The proposed model for low-intensity recording radiation enabled to calculate evolution of the recorded reliefs during holographic recording of gratings. Further improvement of this model was done in [31], where heating of multilayer nanostructure during recording process by high-intensity light and respective

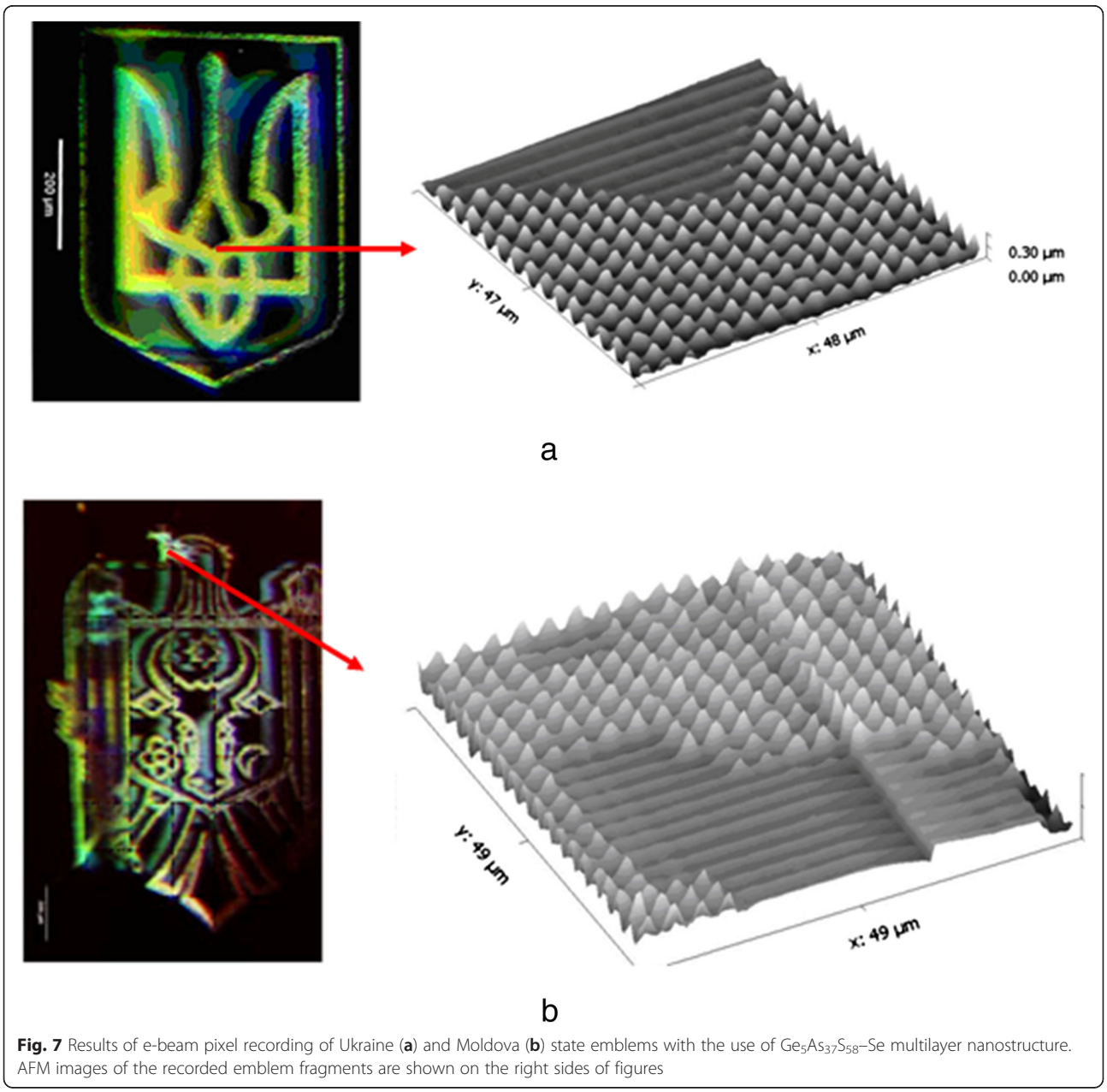

Fig. 7 Results of e-beam pixel recording of Ukraine (**a**) and Moldova (**b**) state emblems with the use of $Ge_5As_{37}S_{58}$–Se multilayer nanostructure. AFM images of the recorded emblem fragments are shown on the right sides of figures

non-linearities of the recording processes were taken into account. Also, it is noted that the thickness change as a result of interdiffusion processes in alternating nanolayers can reach ~5 % values and more. In mechanisms of surface relief formation, it is also necessary to take into account peculiarities of possible surface relief formation in constituent layers of multilayer structure (Se and chalcogenide layer of other composition) [32]. Here, it is necessary to note that mechanisms, processes of mass transfer during surface relief formation, and kinetics of holographic gratings recording in chalcogenide layers and in nanomultilayer structures on the base of chalcogenide glasses are polarization sensitive [32–35].

In Fig. 5, AFM image of surface of holographic diffraction grating with spatial frequency of 1000 mm^{-1}, obtained on the base of $Ge_5As_{37}S_{58}$–Se multilayer nanostructure, is shown.

Under exposure by ion- or e-beams of thin layers of chalcogenide, vitreous semiconductors structural transformations in films are observed [2–5, 36–38]. Shifts of absorption edge or surface deformation under e-beam exposure were observed. With the use of consequent selective etching thin layers of chalcogenide, glasses can be applied in high-resolution lithography processes. It was noted in [36–38] that the effects of stimulated by e-beam thickness increase in separate components of multilayer nanostructure (for example, Se and As_2S_3) are not additive in respect to thickness increase in the same conditions for Se–As_2S_3 multilayer nanostructure. The sum of the thickness increase in separate layers consists of only 30 % from the total measured thickness increase in Se–As_2S_3 multilayer nanostructures. In multilayer nanostructures, it is necessary to take into account also the presence of other processes, for example, formation of As–S–Se. It is supposed that stimulated by light or e-beams processes activate the mentioned processes in such media.

In Fig. 6, AFM images of diffraction gratings recorded by e-beam exposure with 4 and 2 μm periods are presented. Diffraction efficiency of the gratings was ~1 %. Further investigations are necessary for the optimization of multilayer nanostructure parameters and conditions of grating recording.

In Fig. 7a, the results of e-beam pixel recording of the Ukraine state emblem with the use of $Ge_5As_{37}S_{58}$–Se multilayer nanostructure are shown. Image sizes of the Ukraine state emblem consisted of 512×512 pixels (pixel size ~2 μm). AFM image of the recorded emblem fragment is shown on the right side of Fig. 7a. It is necessary to note that at the given recording conditions, pixel height is up to 200–300 nm. Figure 7b shows the results of e-beam pixel recording of the Moldova state emblem with the use of $Ge_5As_{37}S_{58}$–Se multilayer nanostructure. AFM image of the recorded emblem fragment is shown on the right side of Fig. 7b.

Conclusions

Obtained results show that with the use of $Ge_5As_{37}S_{58}$–Se multilayer nanostructures, it is possible to realize direct recording of holographic optical elements (diffraction gratings) and also direct recording by e-beam exposure of diffraction gratings and other surface relief structures.

Competing Interests

The authors declare that they have no competing interests.

Authors' contributions

AS conceived of the study and participated in its design and coordination, fabrication of chalcogenide glasses, results analysis and drafted the manuscript. EA conceived of the study and participated in its design and coordination, results analysis. OP participated in fabrication of chalcogenide glasses, nanomultilayer structures and image recording, studied optical properties, participated in results analysis. AM participated in fabrication of nanomultilayer structures and image recording, participated in results analysis. VA carried out measurement of diffraction efficiency of the gratings. OL carried out the AFM measurements. SS carried out the e-beam image recording. AP participated in fabrication of nanomultilayer structures and image recording. GT participated in fabrication of nanomultilayer structures. All authors read and approved the final manuscript.

Acknowledgements

The research was supported by the project FP–7 SECURE–R21.

Author details

[1]V. Lashkaryov Institute of Semiconductor Physics, National Academy of Science of Ukraine, 41 Nauki ave., Kiev 03039, Ukraine. [2]Institute of Applied Physics, Academy of Sciences of Moldova, 5 Academiei str., Chisinau 2028, Moldova.

Received: 13 October 2015 Accepted: 5 January 2016
Published online: 27 January 2016

References

1. Kostishin MT, Mikhailovskaya EV, Romanenko PF, Sandul GA (1965) About the photographic sensitivity of the thin semiconductor layers. J. Applied and Scientific Photography and Cinematography 10(6):450–451 (in Russian)
2. Mizushima Y, Yoshikawa A (1982) Photoprocessing and lithographic applications. In: Amorphous Semiconductor, Technologies & Devices. Tokyo e.a, Amsterdam, pp 277–295
3. Klabes R, Thomas A, Kluge G, Süptitz P, Grötzschel R (1988) Ion-beam induced silver doping in Ag_2Se/GeSe – resist system. Phys Stat Sol A 106:57–65
4. Saito K, Utsigi Y, Yoshikawa A (1988) X-ray lithography with Ag-Se/GeSe inorganic resist using synchrotron radiation. J Appl Phys 63:565–567
5. Stronski A. Production of metallic patterns with the help of high resolution inorganic resists. Microelectronic Interconnections and Assembly. NATO ASI Series. 3:High Technology, 1998, p. 263–293.
6. Induntyi IZ, Stronski AV, Kostioukevitch SA, Romanenko PF, Shepeljavi PE, Robur II (1995) Holographic optical element fabrication using chalcogenide layers. Optical Engineering 34:1030–1039
7. Stronski AV, Vlček M (2002) *Photosensitive* properties of chalcogenide vitreous semiconductors in diffractive and holographic technologies applications. JOAM 4(3):699–704
8. Stronski A, Vlcek M, Sklenař A, Shepeljavi PE, Kostioukevitch SA, Wagner T (2000) Application of $As_{40}S_{60-X}Se_X$ layers for high efficiency gratings production. J Non-Cryst Sol 266–269:973–978
9. Stronski AV, Vlček M (2000) Imaging properties of $As_{40}S_{20}Se_{40}$ layers. Optoelectronics Review 8(3):263–267

10. Vlček M, Schroeter S, Čech J, Wagner T, Glaser T (2003) Selective etching of chalcogenides and its application for fabrication of diffractive optical elements. J Non-Cryst Sol 326–327:515–518
11. Kovalskiy A, Vlček M, Jain H, Fiserova A, Waits CM, Dubey M (2006) Development of chalcogenide glass photoresists for gray scale lithography. J Non-Cryst Sol 352:589–594
12. Kikineshi S (2001) Light-stimulated structural transformations and optical recording in amorphous nano-layered structures. JOAM 3(2):377–382
13. Kokenyesi S (2006) Amorphous chalcogenide nano-multilayers: research and development. JOAM 8(6):2093–2096
14. Andriesh A, Abaskin V, Achimova E, Prisacar A, Triduh G, Vlček M (2012) Optical properties of nanomultilayers from chalcogenide glasses. 6th Int. Conference on Materials Science and Condensed Matter Physics: abstracts. Chisinau. p. 206.
15. Stronski A, Achimova E, Paiuk A, Abaskin V, Meshalkin A, Prisacar A et al (2015) Surface relief formation in $Ge_5As_{37}S_{58}$–Se nanomultilayers. J Non-Cryst Sol 409:43–48
16. Röling C, Thiesen P, Meshalkin A, Achimova E, Abaskin V, Prisacar A et al (2013) Imaging ellipsometry mapping of photo-induced refractive index in As2S3 films. J Non-Cryst Sol 365:93–98
17. Stronski AV, Vlček M, Tolmachov ID, Pribylova H (2009) Optical characterization of As-Ge-S thin films. JOAM 11(11):1581–1585
18. Tolmachov ID, Stronski AV (2008) Linear and nonlinear optical properties of Ge-As-S films. Proc SPIE 7138:71381X-1-71381X-6
19. Swanepoel R (1983) Determination of thickness and optical constants of amorphous silicon. J Phys E: Sci Instrum 16:1214–1222
20. McClain M, Feldman A, Kahaner D, Ying X (1991) An algorithm and computer program for the calculation of envelope curves. Comput Phys 5(45):45–48
21. Ramirez-Malo JB, Marquez E, Villares P, Jimenez-Garay R (1992) Determinaton of the refractive index and optical absorption coefficient of vapor-deposited amorphous As-S films from transmittance measurements. Phys Stat Sol A 133(1):499–507
22. Marquez E, Gonzalez-Leal JM, Bernal-Oliva AM, Prieto-Alcon R, Ewen PJS, Owen AE (1999) Determination of complex refractive index of thermally evaporated thin films of binary chalcogenide glasses by reflectance measurements. Phys Chem Glasses 40(1):18–25
23. Caricatto AP, Fazzi A, Leggieri G (2005) A computer program for determination of thin films thickness and optical constants. Appl Surf Sci 248:440–445
24. Petkov K (2002) Compositional dependence of the photoinduced phenomena in thin chalcogenide films. JOAM 4(3):611–629
25. Elliott SR (1991) Glasses and Amorphous Materials. In: Materials Science and Technology: A Comprehensive Treatment–Volume 9. VCH, Weinheim, New York, p 376
26. Tauc J, Menth A (1972) States in the gap. J Non-CrystSol 8:569–585, Tauc J. Optical Properties of Amorphous Semiconductors. In: Tauc J, editor. Amorphous and liquid semiconductors. New York: Plenum Press; 1974. p. 159–220
27. Wemple SH, DiDomenico M (1971) Behaviour of the electronic dielectric constants in covalent and ionic materials. Phys Rev B 3(4):1338–1350
28. Wemple SH (1973) Refractive-Index Behaviour of Amorphous Semiconductors and Glasses. Phys Rev B 7:3767–3777
29. Gonzalez-Leal JM (2013) The Wemple–DiDomenico model as a tool to probe the building blocks conforming a glass. Phys Stat Sol B 250: 1044–1051
30. Kikineshi A, Palyok V, Szabo LA, Shipljak M, Ivan I, Beke DL (2003) Surface deformations and amplitude phase recording in chalcogenide nanolayered structures. J Non-Cryst Sol 326–327:484–488
31. Ivan I, Szabo IA, Kokenyesi S (2005) Nonlinear photo-diffusion in amorphous chalcogenide multilayers. Defect and Diffusion Forum Vols 237–240: 1210–1215
32. Tanaka K (2013) Photoinduced deformations in chalcogenide glasses. In: Wang R (ed) Amorphours Chalcogenides. Advances and Applications. Taylor &Fransis group, USA, pp 59–95
33. Teteris J, Gertners U, Reinfelde M (2011) Photoinduced mass transfer in amorphous As_2S_3 films. Phys Stat Sol C 8:2780–2784
34. Gertners U, Teteris J (2010) Surface relief formation in amorphous chalcogenide thin films during holographic recording. Opt Mater 32:807–810
35. Achimova E, Stronski A, Abaskin V, Meshalkin A, Paiuk A, Prisacar A et al (2015) Direct surface relief formation on As_2S_3–Se nanomultilayers in dependence on polarization states of recording beams. Opt Mater 47:566–572
36. Němec P, Takats V, Csik A, Kokenyesi S (2008) GeSe/GeS nanomultilayers prepared by pulsed laser deposition. J Non-Cryst Sol 354:5421–5424
37. Takats V, Nemec P, Miller AC, Jain H, Kokenyesi S (2010) Surface patterning on amorphous chalcogenide nanomultilayers. Opt Mater 32:677–679
38. Takáts V. Photon and electron induced transformations and pattern formation in amorphous chalcogenide nano-layers. Ph.D. Thesis University of Debrecen. Debrecen, 2012.